Front. Struct. Civ. Eng. 2018, 12(1): 26–43
https://doi.org/10.1007/s11709-017-0439-1

RESEARCH ARTICLE

Shanghai center project excavation induced ground surface movements and deformations

Guolin XU[a*], Jiwen ZHANG[b], Huang LIU[b], Changqin REN[c]

[a] *Department of Civil Engineering, Southwest Forestry University, Kunming 650224, China*
[b] *Department of Civil Engineering, University of Kentucky, Lexington, KY 40506-0281, USA*
[c] *Shanghai Geotechnical Investigations & Design Institute Company Limited, Shanghai 200032, China*
[*] *Corresponding author. E-mail: guolin.xu@swfu.edu.cn*

ABSTRACT Empirical data on deep urban excavations can provide designers a significant reference basis for assessing potential deformations of the deep excavations and their impact on adjacent structures. The construction of the Shanghai Center involved excavations in excess of 33-m-deep using the top-down method at a site underlain by thick deposits of marine soft clay. A retaining system was achieved by 50-m-deep diaphragm walls with six levels of struts. During construction, a comprehensive instrumentation program lasting 14 months was conducted to monitor the behaviors of this deep circular excavation. The following main items related to ground surface movements and deformations were collected: (1) walls and circumferential soils lateral movements; (2) peripheral soil deflection in layers and ground settlements; and (3) pit basal heave. The results from the field instrumentation showed that deflections of the site were strictly controlled and had no large movements that might lead to damage to the stability of the foundation pit. The field performance of another 21cylindrical excavations in top-down method were collected to compare with this case through statistical analysis. In addition, numerical analyses were conducted to compare with the observed data. The extensively monitored data are characterized and analyzed in this paper.

KEYWORDS deep excavation, foundation pit, soft clay, top-down method, field observation, ground surface movements, ground deformations

1 Introduction

The upsurge in construction of large scale excavations meeting the increasing demand for underground infrastructure in urban environments is made possible by either the top-down method [1–5] or the bottom-up method [6–8]. Consequently, subsequent or potential impacts on adjacent buildings and underground utilities due to ground movements have received more attention than ever before. A vast amount of field measurements has been obtained regarding performance of excavations. Many empirical or semi-empirical correlations have been developed for predicting excavation deformations based on these field measurements over the last two decades [4,7–15]; however, the most of the excavations were in a rectangular shape or a pattern of strip with area sizes in a plan less than 10,000 m^2 and/or depths less than 30 m. Not much field monitored data is available for skyscraper development involved with the deep foundation pit. Since the performance of an excavation is affected by a complex set of factors that mainly consist of pit size, soil conditions, workmanship, retaining system, and underground water, the validity of these empirical or semi-empirical correlations may not be guaranteed when they are applied to large scale foundation pits. Tan and Wang conducted a series of investigations on the deformation of excavations, induced ground movements, and behaviors of unpropped/multi-propped diaphragm walls based on two large-scale deep foundation pits and rectangular pits peripheral to the main buildings, one of which is the 420.5 m high skyscraper Jinmao Tower (JT), the other of which is 492 m Shanghai World Financial Center (SWFC) [3,8,16,17]. The comparison between the performance of these two foundation pits and a certain number of cylindrical excavations, basement

Article history: Received Jun 4, 2016; Accepted Feb 18, 2017

excavations, and metro station excavations has been conducted in Shanghai soft clay. The central cylindrical shafts of these two skyscrapers were constructed by the bottom-up method by using deep diaphragm walls without bracing struts due to the sufficient spatial arching effect. The Shanghai Center is constructed to be the tallest building in China until 2015 with a topping-out height of 632 m, making it one of the tallest skyscrapers in the world. The excavation provides valuable information regarding the construction of a super foundation pit with an in-plan area of 12,000 m^2 (diameter 123.4 m) and with a depth of 33.7 m. So far, no building which exceeds 600 m in height exists on soft clay except for the Shanghai Center. This project serves as a distinctive case study on the deformation of a super excavation constructed through the top-down method by adopting circular diaphragm walls with six levels of cast-in-situ concrete struts. This information provides a significant guidance for making the performance predictions for similar projects in the future. The ground surface movements and deformations caused by soil type, construction technique, construction sequence, underground water, and retaining structures are emphasized in this paper based on the field measurements.

2 Project overview

2.1 Site conditions

The Shanghai Center was conceived to be a multi-functional and all-around super high-rise building. Fig. 1 presents the site plan view of the foundation pit, and additionally shows the portions of the annexes and surrounding high-rises. It is located at the most congested area, Lujiazui Finance and Trade Zone, in Shanghai and is bounded by the intersections of Central Yincheng, Garden Stone, Circle Lujiazui, and East Tai Streets, with a distance of 96 m away from the central cylindrical shaft of JT on the north side and a distance of 107 m away from the core-tube of SWFC on the east side. In addition, this area is surrounded by complicated underground pipelines and underground facilities, including Metro Line 2 in service

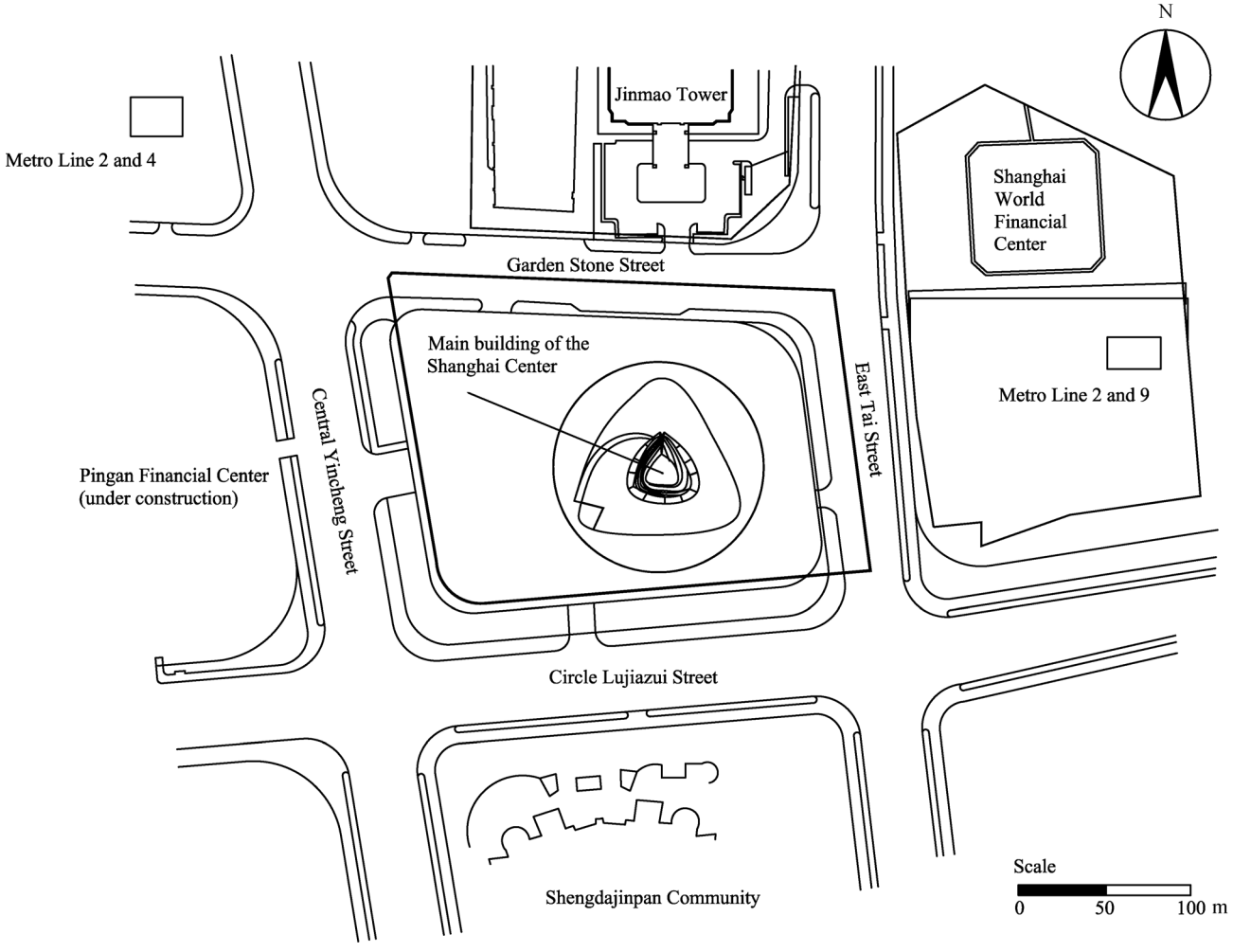

Fig. 1 Site location and adjacent structures

and Line 14 in construction on the north side, as well as Metro Line 2 and 9 in service on the east side. As explained by Tan and Wang when the diameter of a cylindrical shaft exceeds 90 m, both the ring stiffness and spatial arching effect would be impaired significantly [8]; thus, due to the weak spatial arching effect, it is extremely difficult to maintain retaining walls in a circular shape without support. This project involved the construction of a circular foundation pit which was constructed in an open multi-strutted excavation with a diameter of 123.6 m adjacent to several rectangular annex foundation pits. The whole foundation pit was comprised of two parts: the central pit and the peripheral pit. The excavation of the peripheral pit using the bottom-up method would be started after the underground facilities of the central pit completed by using the top-down method. This paper focuses on the observed performance of the central deep foundation with respect to lateral diaphragm wall movements, the ground settlements, and pit basal heave.

The site was previously occupied by Lujiazui Golf Course which contributed negligible net surcharge to the foundation soils. Prior to construction, Shanghai Geotechnical Investigations and Design Institute Company Limited (SGIDI) was appointed to conduct a comprehensive investigation regarding subsurface conditions and soil parameters. Fig. 2 illustrates the stratified soil layers at the site with the dimension of the foundation pit. The site is primarily composed of saturated clay, silty soil, and sandy soil, which are distributed in stratification. The borehole observation indicated that the site mainly consisted of fourteen layers, among which layer 8 was not detected according to unified strata of Shanghai soft clay made by Shanghai Construction and Management Commission (SCMC) [18,19]. The cast in place (CIP) concrete piles, with lengths of 52 to 56 m, were evaluated and chosen due to their high strengh and low construction cost. Only nine layers of compressible sands and clays, which alternated to a depth more than 110 m, were illustrated and considered as supporting layers providing frictional resistance. The main excavation portion, above the depth of 24 m, was dominated by cohesive soil characterized by high moisture content, high void ratio, high sensitivity, high compressibility, and low intensity. Both of the field tests (e.g., borehole observation, cone penetration test, vane shear test, dewatering test, and pressure meter test) and laboratory tests (e.g., consolidation test, compression test, and triaxial test) were carried out to obtain the site information. The variations of some important soil properties in average value along the depth are shown in Fig. 3. Granite as the bedrock was embedded 270 m below the ground surface, which was far beyond the reach of practical foundations. Bearing piles of the core tube reached a depth of 80 m where layer 9_{2-1} of the dense silty sand was the bearing stratum. The phreatic water table fluctuates seasonally in elevations ranging from 0.75 to 3.9 m. The first and second aquifer (artesian water) was encountered at layer 7 with an average depth 30 m and layer 9 with an average depth 70 m, respectively. These two aquifers were connected with one another for a total thickness around 97 m. Sustainable and stable dewatering on-demand to lower level of the hydraulic pressure is a significant and challenging factor that impacts the safe and smooth construction of the foundation pit due to the complicated underground water conditions.

2.2 Construction procedure of the foundation pit

The top-down method was adopted to conduct the excavation of the central foundation pit which was supported by 50 m deep diaphragm wall with six levels of in situ concrete struts that correspond to six levels of excavation. The six-level excavation is based on the principle of the symmetrical, balanced, and layered excavation procedure. The whole excavation was divided into ten stages involving numerous tasks over a span of 14 months. The detailed information of each stage is summarized in Table 1. Except for level one excavation, the soils along the designed circumferential walls were dug out first and placed in the center of the site prior to removal, following the immediate manufacture of walls and strut framework and the casting of walls with struts. The soils at the center of the pit would be removed after the walls' concrete at each level gained 80% concrete strength, then the next level of excavation would be initiated. Four lift platforms were built separately at north (No. 1), south (No. 2), west (No. 3), and east (No. 4) along the pit circumference for transferring soil, instruments, materials, and workers, which greatly facilitated the construction of the foundation pit. Circular diaphragm walls with high stiffness aiming to waterproof were adopted as the retaining walls, as well as the basement exterior walls. Prior to the first level excavation, a circular capping beam (CB) was built along the top of the diaphragm walls for the purpose of strengthening the vertical stiffness of the retaining structure. The whole circular diaphragm walls consisted of 70 panels, each of which would be constructed synchronously for the same level and connected without crevices except for construction joints. A uniform size of 176 m (length) $\times$ 1.20 m (thickness) was adopted, and a distance of 61.77 m between the turning place (connection between two panels) and the circle center of the pit was implemented for each panel. The six lateral levels of struts were concatenated by vertical columns for the purpose of making them perform together as well as fortifying the retaining system. The size of the struts is presented in Table 2. To accommodate the hazard of pit collapse caused by the inrushing of artesian water, pumping wells were installed along the pit circumference to reduce the water pressure by the dewatering that spanned from November 22, 2009 to April 5, 2010. The field recorded data demonstrates that smooth and fitting ground surface movements and ground deformations caused by symmetrical, balanced, and

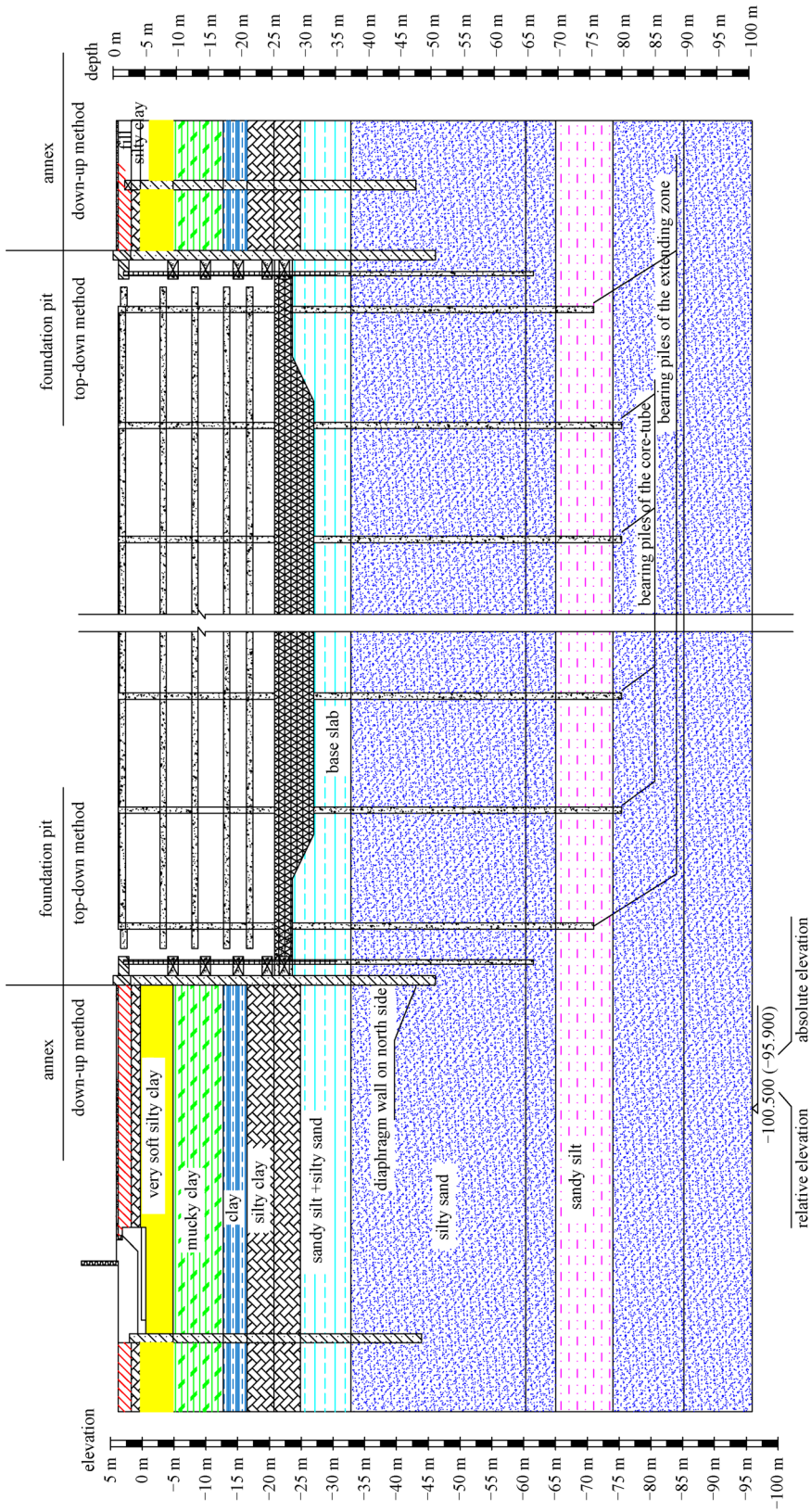

Fig. 2 Cross section of the foundation pit with the soil profiles

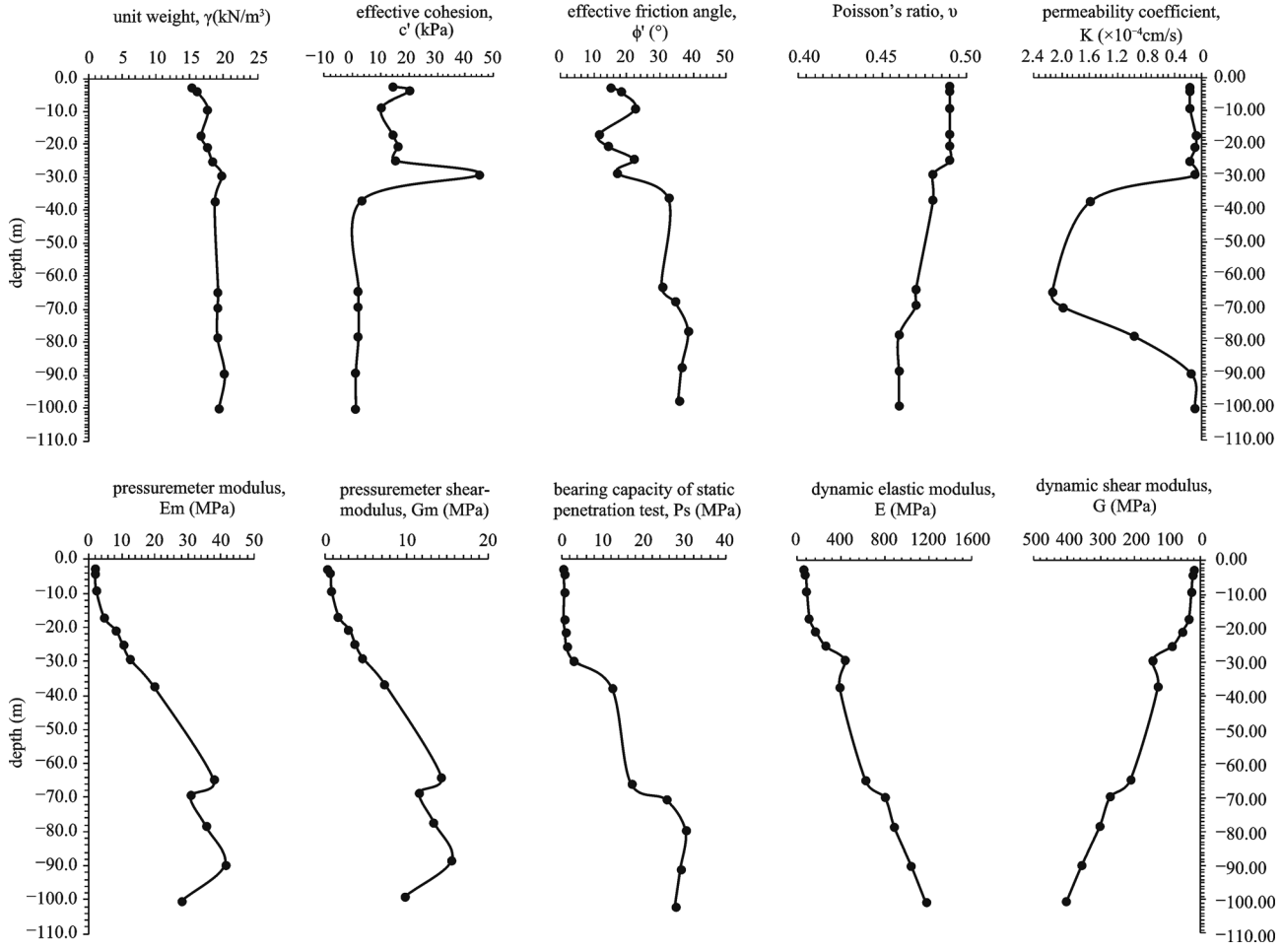

Fig. 3 Soil properties along the depth at the site

layered excavation procedure for deep circle pits could produce minimal adverse impact on retaining system.

2.3 Instrumentation

An extensive instrumentation program was undertaken alongside the foundation pit as well as the internal/peripheral soils to monitor the performance of the retaining systems, ground movements, and underground water. The monitoring system consisted of two categories based on different properties: one involves monitoring points where the monitoring facilities were anchored to structure parts, the other one refers to boreholes where monitoring facilities were placed in polyvinyl chloride (PVC) pipes or tubes. Fig. 4 shows the instrumentation layout of the boreholes and the monitoring points in the plan. The location and quantity of the monitoring facilities/items were determined by a series of factors (e.g., construction technology, the excavation depth, sequence, and observation objects), which attempt to arrange different monitoring facilities/items on the nearby locations or in the same soil profiles in consideration of facilitating the comparisons between different field measurements. The instrumentation used to monitor the ground surface movements and deformations for the foundation pit included:

1) Lateral movements of the diaphragm walls were measured by sixteen inclinometers (P01~P16) that were anchored to the reinforcement cages at an elevation of 45 m below the ground surface, among which inclinometer tubes P13 and P15 were damaged during the concreting.

2) Lateral movements of the peripheral soil were measured by fifteen inclinometers (T01~T15) that were placed in boreholes with an average depth of 60 m, and these boreholes were approximately 1.5 m behind the diaphragm walls.

3) Standpipes were installed inside (NS1~NS4) and outside (WS1~WS8) of the pit to observe phreatic water table, and observation wells were drilled inside (NY1~NY3) and outside (WY1~WY4) of the pit to observe the artesian water levels.

4) Subsurface settlement outside of the pit was measured by a settlement magnetic system (RI~R8) individually placed in boreholes with an interval of 5 m from the elevation –2.0 m along the depth.

Table 1 Main stages of the construction of the central foundation pit

Stage	Operation	Activity	Day
1	The first level strut (Elevation −1 to −8.5 m)	• Construct the first level wall and retaining structure framework with 1 m height as preparation work; 07/27/2009–08/24/2009 • Cast concrete; 08/25/2009–08/27/2009	53
2&3	The Second level strut (Elevation −8.5 to −14.5 m)	• Remove the first level soil to form a pit with a size of 50m (length) × 15m (width) × 5m (depth) around the lift platform No. 1; 09/16/2009–09/22/2009 • Excavate to the bottom of the second level strut with a depth of 10 m around the lift platform No. 3 in a direction of north-south from peripheral to central; 10/05/2009–10/11/2009 • Change excavation sequence, excavate in the direction of east-west from central to peripheral;10/11/2009–10/23/2009 • Construct the second level wall and retaining structure framework and cast concrete; 10/24/2009–10/30/2009	45
4	The Third level strut (Elevation −14.5 to −19.5 m)	• Excavate to the third level along the circumference but do not remove the central soil; 10/31/2009–11/03/2009 • Construct the third level wall and retaining structure framework and cast concrete; 11/04/2009–11/16/2009	18
5	The Fourth level strut (Elevation −19.5 to −24.0 m)	• Remove the central soil at the third level; 11/17/2009–11/21/2009 • Begin to dewater; 11/22/2009 • Excavate along the circumference to the fourth level but do not remove the central soil; 11/22/2009–11/29/2009 • Construct the fourth level wall and retaining structure framework and cast concrete; 11/30/2009–12/07/2009 • Remove the central soil at the fourth level; 12/08/2009–12/14/2009	28
6	The Fifth level strut (Elevation −24.0 to −28.0 m)	• Excavate along the circumference to the fifth level but do not remove the central soil; 12/15/2009–12/20/2009 • Construct the fifth level wall and retaining structure framework and cast concrete; 15/21/2009–01/04/2010	14
7	The Sixth level strut (Elevation −28.0 to −33.7 m)	• Remove the central soil at the fifth level; 01/05/2010–01/08/2010 • Excavate along the circumference to the sixth level but do not remove the central soil; 01/09/2010–01/23/2010 • Construct the sixth level wall and retaining structure framework and cast concrete; 01/24/2010–01/30/2010	25
8	Cast concrete under-layer	• Remove the central soil at the sixth level and excavate to −33.7m; 01/31/2010–02/03/2010 • Cast all concrete under-layer; 02/04/2010–02/12/2010	9
9	Base plate construction	• Construct the base plate framework and cast concrete; 02/08/2010–04/19/2010 • End dewatering; 04/05/2010	71
10	Underground Construction	• Construct the underground structure and facilities; 04/20/2010–09/29/2010	161

Table 2 Size and location of the struts

Level	Size, height × thickness (mm × mm)	Central elevation (m)
1	3700 × 1500	−1.75
2	2800 × 1500	−9.30
3	2800 × 1600	−15.30
4	3000 × 1600	−20.30
5	3000 × 1800	−24.90
6	3000 × 1800	−28.90

5) Pit basal heave was recorded by four arrowhead magnets (C1~C4) at four platforms and two arrowhead magnets (C5 and C6) at the center of the pit from the elevation −32.0 m with an interval of 5 m.

3 Field performance

3.1 Walls and circumferential soil lateral movements

The walls' lateral movements at P01 and P05, which are selected as typical measured sections, are summarized in Fig. 5. P01 was located at the north side and P5 at the east side. The lateral movement variations of the walls both along the depth and the excavation progress are separately illustrated. It is noticed that the lateral movements of the walls at these two points from stage 1 to stage 10 developed into a bulged profile moving toward the excavation side. However, during the casting of the base slab, both the retaining walls and the soils began to change the moving direction from inward (excavation side) to

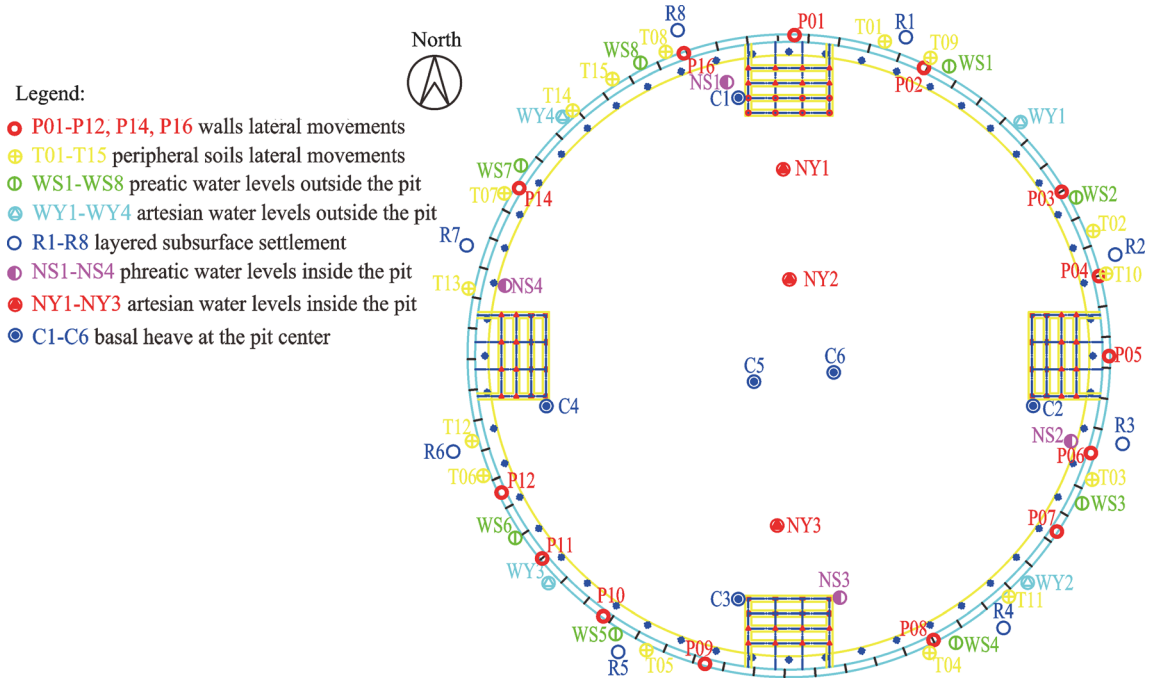

Fig. 4 Instrumentation layout of the circular pit

outward (ground side). Subtle outward displacement was found for the walls during stage 10. This reverse implies that the underground structures (e.g. base slab, basement) could play a role on restraining both retaining walls and ground moving inward. Such a phenomenon was also reported by Moormann and Tan and Wang [3,12]. The maximum lateral movement of the walls at P9 was 73.48 mm, the smallest one among all observation boreholes, while the maximum lateral movement of the walls at P11 was 97.2 mm. This discrepancy can be attributed to several factors: (1) P09 was near the lift platform No.2, and the deflection was suppressed to a certain extent due to the strengthened vertical stiffness of the walls because of the existence of the CIP piles that were used to support the platform; (2) P11 located at the driving zone of heavy trucks, which could increase the lateral load imposed on the walls; and (3) the joint between the wall panel W43 and T05 was designed as a casing connection, which is usually perceived as low integrality.

The characteristics of the lateral movements of the walls at different depths could be examined by placing monitoring instruments in the vertical walls along the depth. By averaging all observation boreholes, the walls' maximum lateral movement (δ_{hm}) was 78.3 mm, which occurred at a depth (H_m, where δ_{hm} occurred) of 18 m below the ground surface that is equivalent to the excavation depth 33.7 m (H) of this foundation pit. Many researchers have statistically analyzed the relationship between the maximum lateral movement of the walls and the excavation depth. Compared with the behaviors of the retaining walls for the deep excavations in soft soils worldwide, $\delta_{hm} = 0.23\%H$ this study is far below the upper boundary $\delta_{hm} = 1.0\%H$ [25] and also below $\delta_{hm} = 0.5\%H$ [20] or $\delta_{hm} = 0.6\%H$ [21]. Liu and Lee et al. reported that the maximum wall deflections of some excavations occurred below the excavation bottom due to the thick layer of soft soils embedded below the excavation bottom [22,23]. Their conclusions were based on shallow excavations and cannot explain the changes of location of the walls' maximum movement for deep excavations. In this case, H_m (18 m) was examined above the excavation bottom (33.7 m). Regarding deep excavations in soft soils, the highly-strengthened support system and/or the shorter distance from excavation bottom to stiffer bearing strata may make the maximum wall deflection occur above the excavation bottom. This study $H_m = H - 16$ matches well with the rule that most H_m ranged from $H_m = H - 20$ to $H_m = H + 12$ for cylindrical excavations in Shanghai soft clay by using the top-down method [3].

Tan and Wang proposed a linear equation ($\delta_{hm}/H = 1.5 \times 10^{-5} D$) to describe the relationship between the maximum lateral movement of the walls (δ_{hm}) and central pit diameter (D) [8]. The calculated δ_{hm} by using this equation for this study is 62.4 mm, which is smaller than the actual observed value 78.3 mm. This discrepancy might arise from several reasons: (1) this equation is a linear regression based on some cases that the shaft diameters are less than 90 m, while the diameter in this study is 123.4 m; (2) most cases that were used to infer this equation are less than 20 m in excavation depth; and (3) circular deep excavations with smaller diameter usually tend to deform less due to the spatial arching effect.

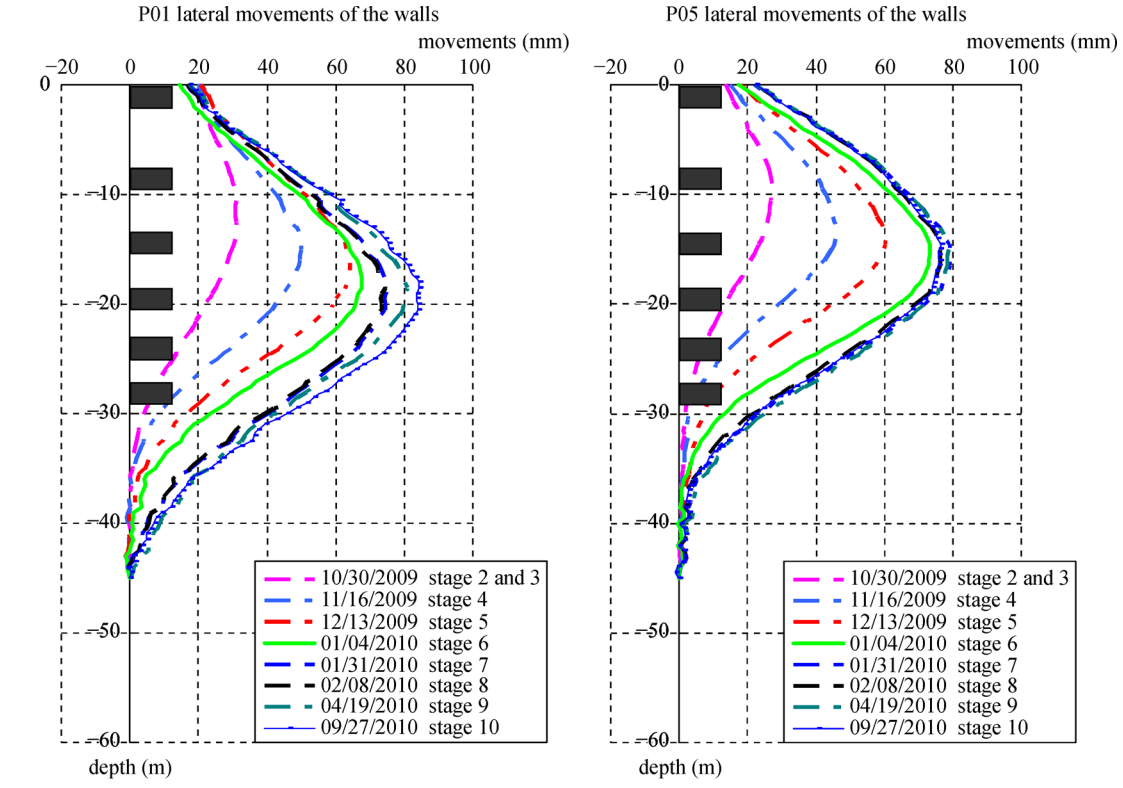

(a)

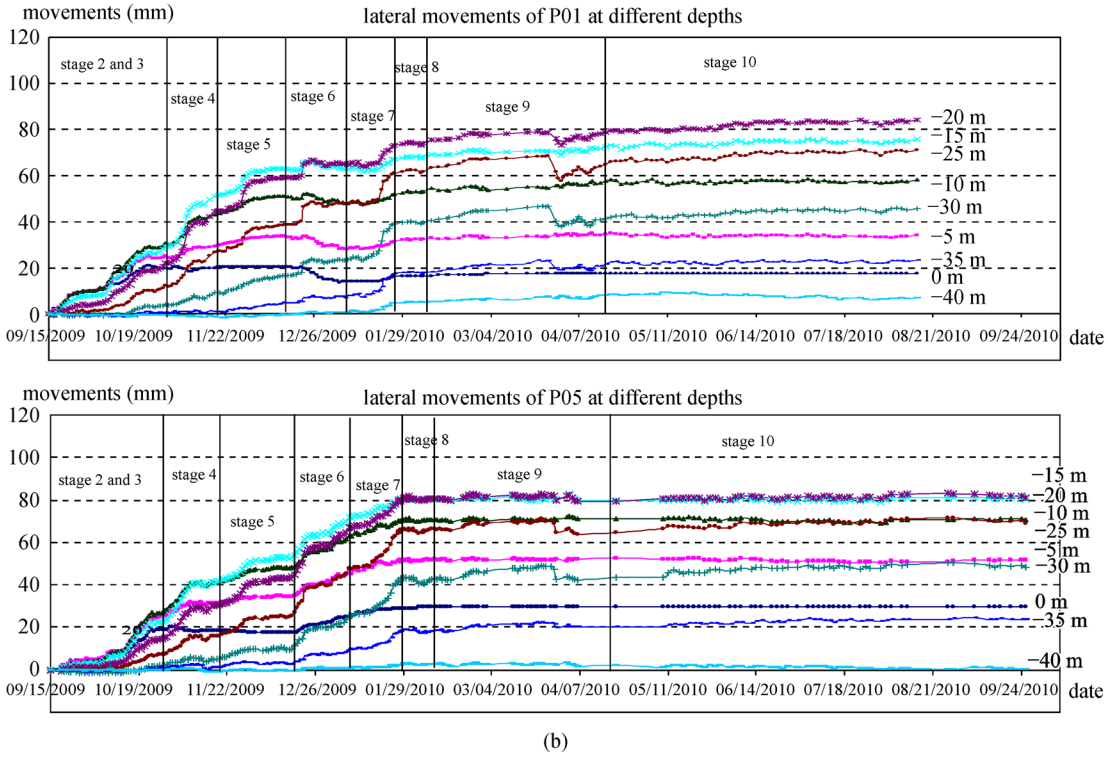

(b)

Fig. 5 Lateral movements of the walls at P01 and P05: (a) variations in different stages along the depth; (b) variations at different depths along the excavation progress

No toe movement of the retaining walls was found by screening the inclinometers in the walls. Liu et al. considered the ratio of embedded length of retaining walls (H_d) to the excavation depth (H) as a significant fator that may contribute to toe deformation, and a large embedment ratio between 0.7 and 0.94 could help to impede the formation of toe deflection [24]. However, Wang et al. concluded that no necessary correlation exists between embedment ratio and wall maximum lateral deflection by conducting a statistical analysis regarding the recent excavations in Shanghai soft soils [14]. The embedment ratio of Shanghai Center is consistent with the conclusion of Wang et al. that an increase in the embedment ratio would not produce a corresponding decrease in maximum wall movement if the stability of the excavation had been ensured. The embedment ratio for Shanghai Center was 0.49, which was much smaller than the lower boundary 0.7 or the average value 0.96 for diaphragm walls in Shanghai soft soils [14]. The lack of toe deflection detected with this irregular ratio might be ascribed to the high stiffness of the retaining walls supported by six level struts to guarantee the stability of the excavation.

The lateral movements of the circumferential soil behind walls were also monitored. By examining the recorded data, the soil lateral movements showed a deflection pattern similar to the lateral movements of the walls. Due to the similar variation trend, the measurements of the circumferential soil movements will not be presented here. The maximum lateral movement of the circumferential soil, δ_{hS}, was 79.4 mm in average, which occurred at 17 m below the ground surface. The development of the walls and circumferential soil lateral movements mainly took place from stage 2 to 7 with the average accumulative lateral movement of 73.2 mm (93% of the maximum) and 72.4 mm (91% of the maximum) for the diaphragm walls and the circumferential soil, respectively. From stage 8 to stage 10, the wall and the soil lateral movements tended to decrease, and the location where the maximum lateral movements were measured moved gradually downward.

3.2 Peripheral soil vertical movements in layers and ground settlements

The magnetic system used to monitor the layered vertical settlements of peripheral soil at different depths was comprised of eight sections (RI~R8), each of which was located, respectively, at an elevation from −6 m to −56 m with an interval of 5 m. Hence, the whole site was divided into eleven layers. These eleven monitoring spots were installed 3 m behind the walls. Table 3 summarizes the accumulative vertical movements and the average vertical movements of each section at the end of the excavation. R1 and R5 are selected to illustrate the variations of layered vertical movements in different excavation stages and at different depths, which are presented in Fig. 6 (a) and Fig. 6 (b), respectively.

The layered vertical movements of the soils outside of the pit are affected by stress relief (soil removal), ground lateral movements, and dewatering. The monitoring spots at different depths displayed different vertical movements; the soils above −30.0 m tended to settle, and the settlement decreased with the increase of the depth, while the soils below −30.0 m presented a heave tendency, and the heave increased with the depth. The maximum layered soil settlement (δ_{vm}) was 58 mm, observed by R5 at a depth of −6 m. The extreme trend line between the maximum soil settlement and the excavation depth is $\delta_{vm}/H = 0.172\%$ for this study, which falls into the range suggested by Clough and O'Rourke: the upper line $\delta_{vm}/H = 0.5\%$ and the lower line $\delta_{vm}/H = 0.15\%$ [20]. The average trend line of this study $\delta_{vm}/H = 0.142\%$ is also within the range between $\delta_{vm}/H = 0.05\%$ and $\delta_{vm}/H = 0.2\%$ proposed by Hashash et al. based on the medium stiff Blue Clay of Boston [7]. Large settlements over 40 mm were found at the depth of −6 m and −11 m, while the monitoring spot at −26 m showed 10 mm settlement. The faster growth in heave was recorded between −31m and −46 m, but the heave growth slowed down below −46 m. On the other hand, the monitoring spots at the same section also exhibited different vertical movements in different stages. Similar deflection pattern was found for section R1 and R5: (1) heave changed slightly for monitoring spots below −16 m from stage 2 to stage 5, but increased rapidly during stage 6 to stage 8, and then stabilized to a fixed value after stage 9; (2) slight vertical movements occurred throughout the excavation for monitoring spots between −16 m and −41 m; and (3) settlement increased from stage 2 to stage 8 for monitoring spots above −16 m, and then reached a steady state in the construction of underground structures and facilities during stage 9 and 10. By examining the monitoring spots which showed settlements, the maximum settlement 60 mm was detected at −21 m of section R5. This result is in agreement with the maximum lateral movement of the retaining walls.

During stages 2, 3, and 4, the peripheral soil vertical movements were mainly controlled by stress relief (soil removal) and lateral movements of the ground. After the dewatering began in stage 5, the vertical movements of the soils above −21 m can be classified as settlement, but soils behaved as heave below −21 m. During stages 6 and 7, the peripheral soil below −31 m rebounded obviously. During stages 8, 9, and 10, soil deflections (settlement/heave) gradually stabilized, but little heave took place after the end of the dewatering on April 5, 2010. The recorded layered vertical movements of the peripheral soil indicate that the excavation exerted an influence on the heave of soils below the excavation bottom (−33.7 m).

The ground vertical movements of the four surrounding streets (Central Yincheng, Graden Stone, Circle Lujiazui, and East Tai Streets) were monitored and the results are shown in Fig. 7. In general, the ground vertical movements

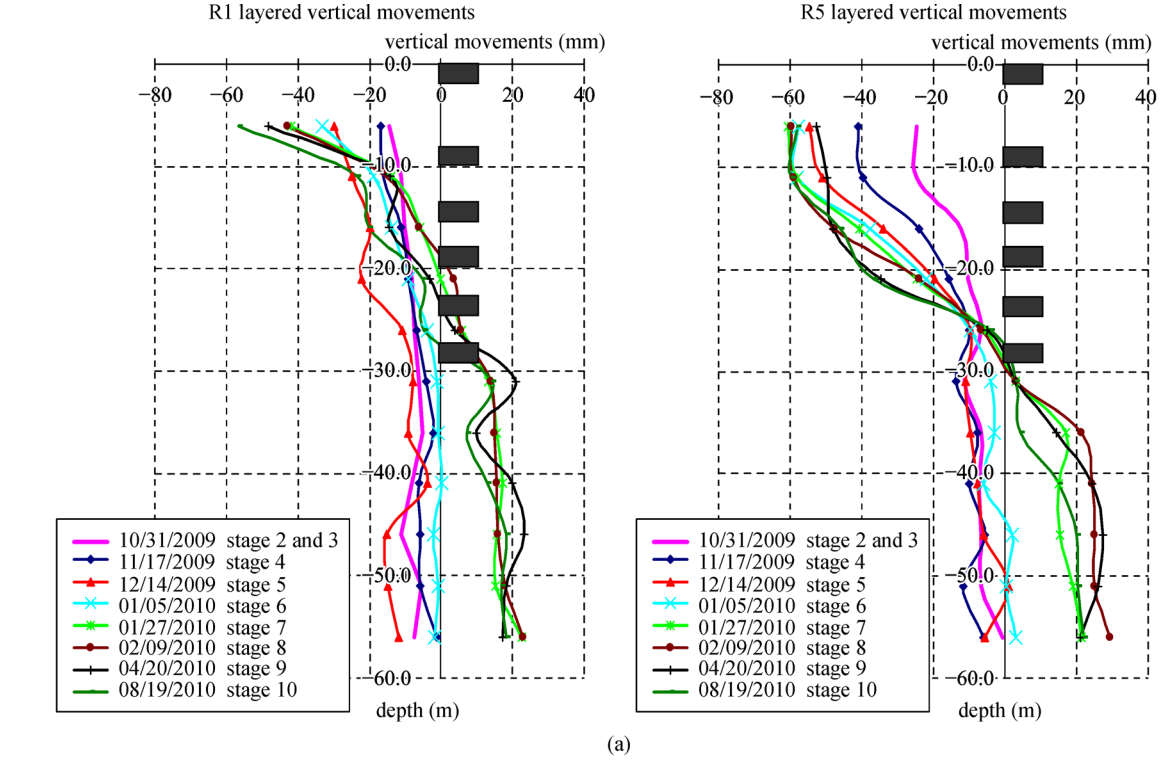

(a)

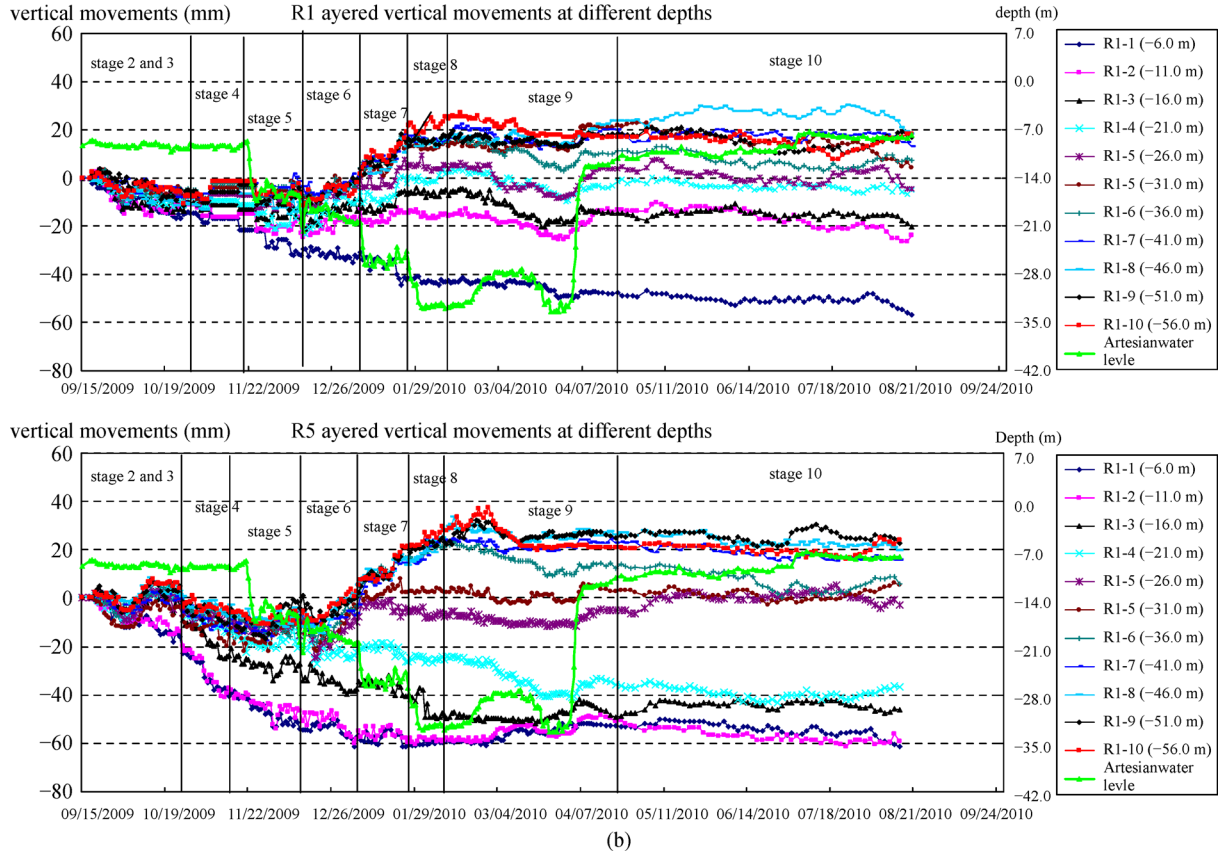

(b)

Fig. 6 Vertical movements of the peripheral soil in layers at R1 and R5: (a) variations in different stages along the depth; (b) variations at different depths along the excavation progress

Table 3 Layered vertical movements of the soils behind the walls at different depths at the end of the excavation

depth (m)	accumulative settlement (mm)								average (mm)
	R1	R2	R3	R4	R5	R6	R7	R8	
−6.0	−57	−48	−49	−49	−58	−46	−41	−41	−48
−11.0	−24	−41	−48	−48	−60	−42	−44	−39	−42
−16.0	−20	−19	−41	−41	−46	−38	−38	−29	−33
−21.0	−5	−7	−29	−29	−37	−27	−27	−17	−21
−26.0	−5	4	−20	−20	−4	−4	−7	−12	−7
−31.0	4	10	−5	−5	3	−2	−5	1	1
−36.0	7	9	8	8	4	4	2	−2	5
−41.0	13	19	12	12	15	7	−1	4	10
−46.0	18	15	15	15	20	12	9	3	13
−51.0	17	10	13	13	20	17	17	3	14
−56.0	18	16	20	20	22	18	19	10	18

Note: Negative denotes settlement; positive denotes heave.

presented settlements that were dually affected by the soil removal and dewatering. The rate of settlements varied in different stages. During stages 2, 3, and 4, the rate decreased with the increase of the distance between the street and the central pit. The ground near the annexes settled more than the aforementioned streets, and small settlements were perceived on the surface of these four streets. With the growth of the excavation depth and initiation of the dewatering from stage 5 to 7, the ground settle rate significantly increased. The influence scope of the excavation expanded and a funnel-shape was developed in the settlement profile. The maximum ground settlement was found at a distance of 20 m from the annex. In stage 8, the ground vertical movements of these four streets were hardly affected by the excavation. Due to the end of the dewatering and the construction of base slab during stage 9 and 10, the ground tended to rebound while the heave rate was smaller than the settle rate.

3.3 Pit basal heave

Soil removal during excavation would directly cause the basal soils to rebound. Six groups of arrowhead magnets were used to monitor the basal heave. In each group, six arrowhead magnets were placed at depths of −31 m, −36 m, −41 m, −46 m, −51 m, and −56 m to measure the different heave amounts. Fig. 8 shows the recorded data of the heave amounts along the depth for all arrowhead magnets.

Before stage 4, the basal heave increased obviously due to the soil removal. After the dewatering began (stage 5), the soils above the artesian water level started to consolidate. The heave increased slowly, and sometimes behaved as settlement (i.e. C1 at the depth of −46.0 m) caused by consolidation which was larger than the heave. At the end of the excavation (stage 9), the heave gradually stabilized. In stage 10, the heave measurements did not take into account the settlement caused by the construction of the base slab and other underground structures.

The heave changed consistently with the excavation levels: the heave amounts increased when the soils were removed while decreased when the diaphragm walls and the struts were completed in each level. This corresponds to the conclusion that the stress relief would cause the basal soil to rebound while the retaining walls would suppress the soils moving toward the pit behind the walls. The vast subsurface beneath the excavation bottom was involved to generate a heave amount which was characterized by a decreasing tendency along the depth. For the arrowhead magnets at the center pit (C5 and C6), the measured heave amounts at −56 m of the both boreholes were higher than 35 mm, thus assuming that a great thick subsurface below the excavation bottom would rebound. The maximum basal heave amounts, δ_{bh}, that were measured at C5 and C6 are used to identify the relationship between the maximum basal heave and the excavation depth, H. The range of the measured maximum basal heave in this excavation between $\delta_{bh} = 0.15\%H$ and $\delta_{bh} = 0.16\%H$ is much lower than the range between $\delta_{bh} = 0.3\%H$ and $\delta_{bh} = 0.9\%H$ that was proposed by Tan and Wang based on a certain amount of basement excavations in Shanghai soft clays [8]. In addition, the relationship between the maximum basal heave, δ_{bh}, and the excavation diameter, D, was described as $\delta_{bh} = 0.04\%D$.

Fig. 9 describes the relationship between the heave amount and the distance from the center of the pit to the measured points. It can be seen that the heave amounts at the center were higher than the periphery because the weight of the diaphragm walls and the struts could partially compensate the soil removal. In general, the basal heave might result from a comprehensive function of multiple factors: (1) rebounding due to soil removal;

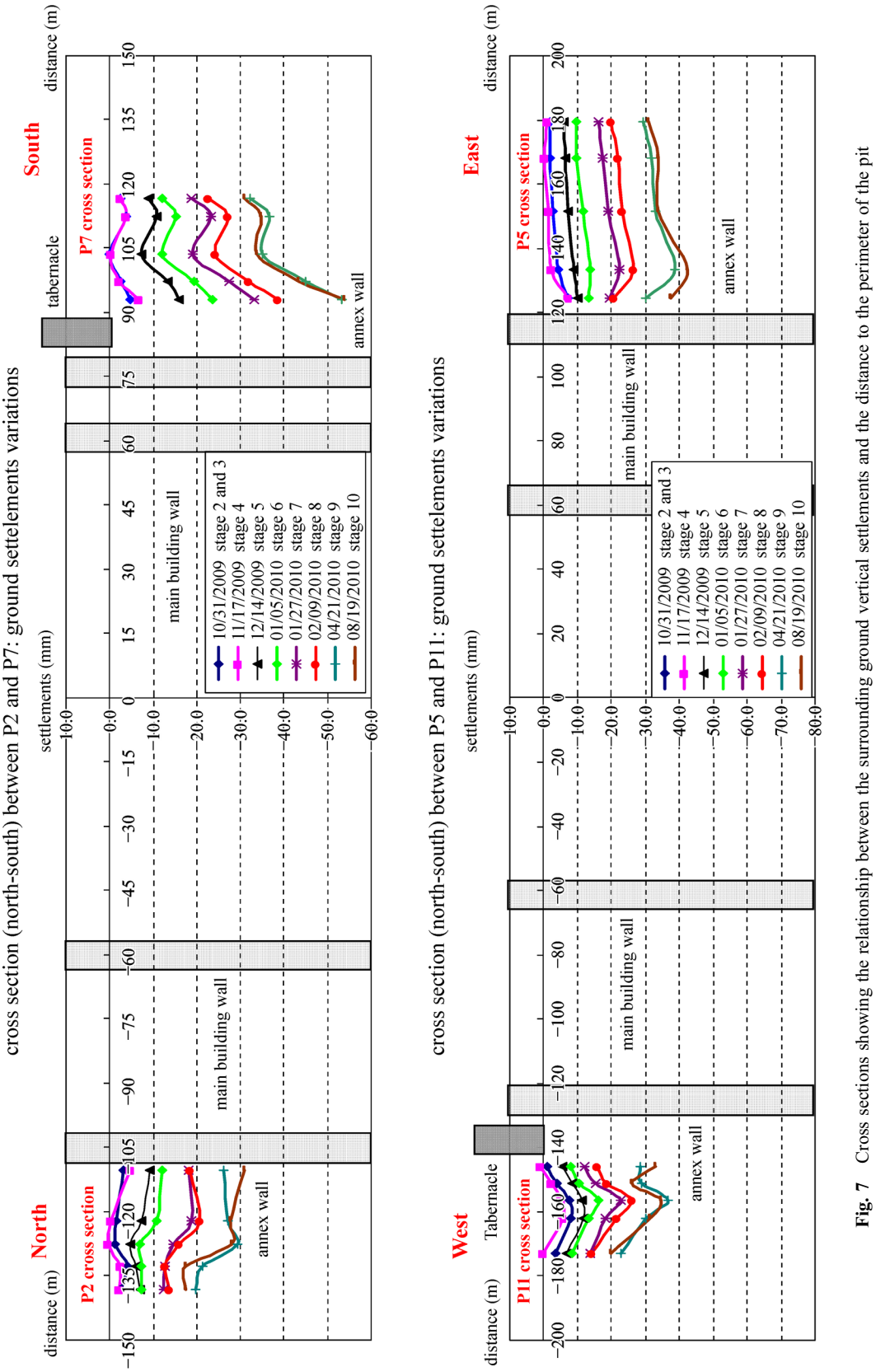

Fig. 7 Cross sections showing the relationship between the surrounding ground vertical settlements and the distance to the perimeter of the pit

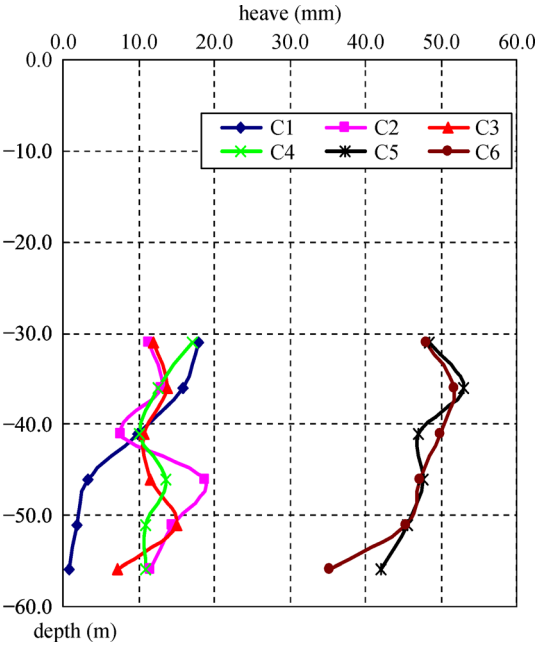

Fig. 8 Basal heave along the depth for all arrowhead magnets

(2) consolidation induced by discharging of artesian water; (3) suppression from soils outside of the pit; and (4) squeezing by retaining walls.

4 Comparison with previous deep excavations in Shanghai

A database comprising 21 individual cylindrical excavations in top-down method was collected through Chinese journals, conference proceedings, master and doctor theses, and monographs to identify the relationship between excavation depth H (or foundation pit diameter D) and maximum lateral wall movement δ_{hm} , maximum layered soil settlement δ_{vm}, and maximum basal heave δ_{bs}, respectively, as well as to compare this case to the previous deep excavations in Shanghai. In order to see the variation tendency between the embedded depth ratio (H_d/H) and δ_{hm}, δ_{hm}, and δ_{bs} individually, charts of scatter with smooth lines were established. The observed values of δ_{hm} δ_{vm}, and δ_{bs} for Shanghai Center are generally below the average values of the given database. The value of H_d/H for this care is 0.49, which is almost the same with another three cylindrical excavations whose the values of excavation depth are around 30 m.The analysis in Fig. 10 and Fig. 11 exhibits the following features:

- There is a clear tendency that the embedded depth ratio (H_d/H) decreases with increasing the excavation depth for cylindrical excavations in top-down method. This case can be used to verify the fact that the stiffness of support system for deep excavations would be greatly enhanced that could mitigate the overturn risk caused by inadequate embedded depth. Therefore, further increase of the embedment length of the walls has a limited influence on the performance of the excavation. This result can provide design engineers an economical relevance for the design of deep excavations in soft clays.
- The depth where the maximum lateral wall movement (δ_{hm}) occurred would increase as the excavation depth increases. Values of H_m generally range from $H+6$ to $H-8$ with an average value of $H-1.02$ for this database.
- From Fig. 10(c), these results including maximum lateral wall movement (δ_{hm}), maximum layered soil settlement (δ_{vm}), and maximum basal heave (δ_{bs}) would increase as the excavation depth increases. The average values of δ_{hm} δ_{vm}, and δ_{bs} are $0.28\%H$, $0.21\%H$, and

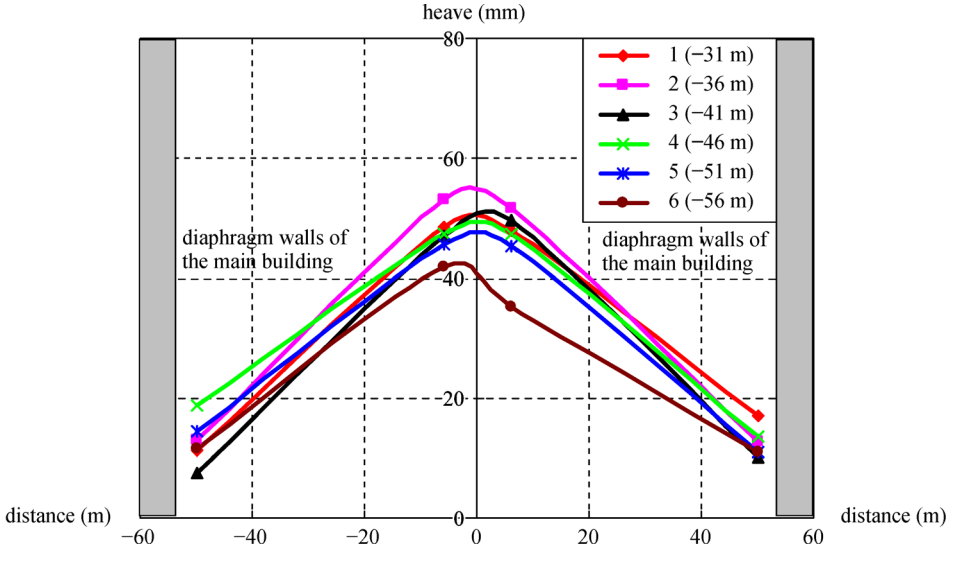

Fig. 9 Relationship between the heave amount and the distance from the center of the pit to the measured points

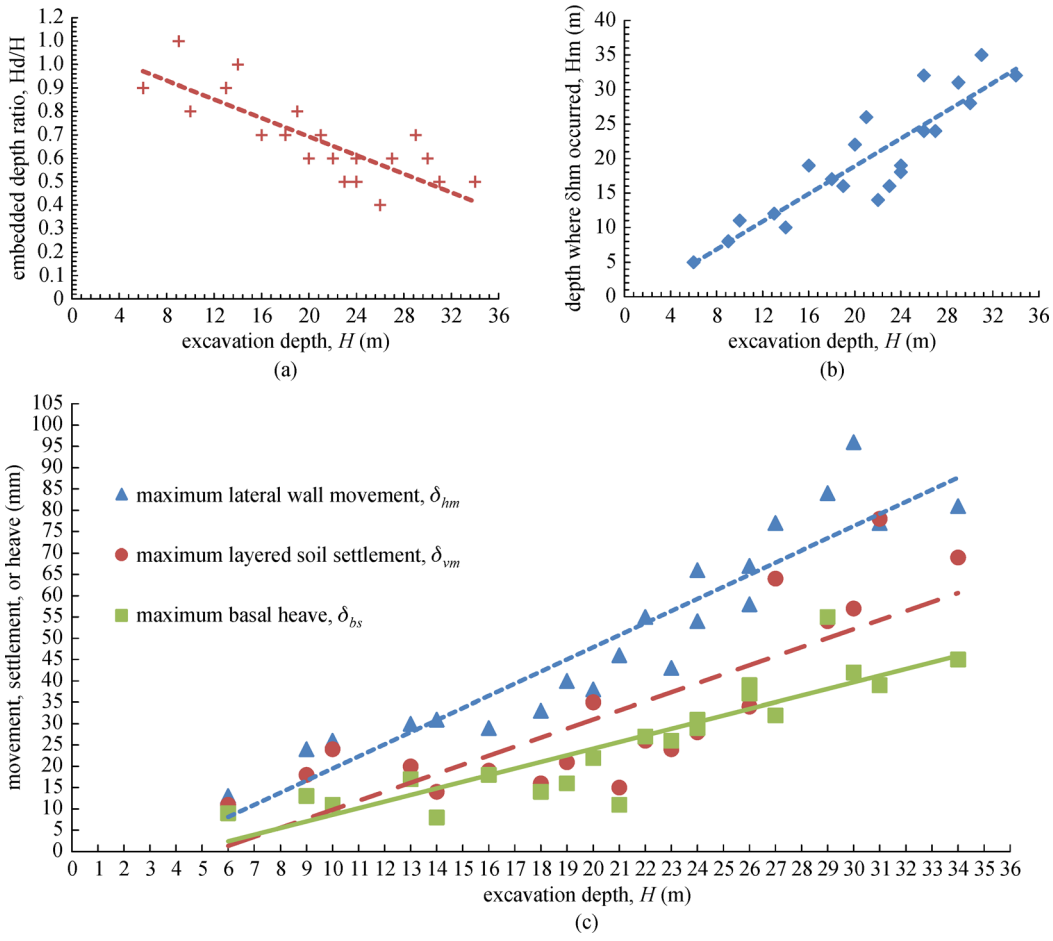

Fig. 10 Embedded depth ratio H_d/H versus H ; (b) depth where δ_{hm} occurred versus H ; (c) relationship between H and δ_{hm} , δ_{vm}, and δ_{bs}, respectively

0.16%H , respectively. These three values for this case are in close proximity to the results of the database.

• No obvious relationship exists between embedded depth ratio (H_d/H) and foundation pit diameter (D). It seems that the foundation pit diameter is independent of the embedded depth ratio. A relationship $H_m = 0.21\%D$ reflects that the depth where H_m occurred increases with increasing the foundation pit diameter.

• For all maximum lateral wall movement, maximum layered soil settlement, and maximum basal heave tend to increase as foundation pit diameter increases. The average values of δ_{hm} δ_{vm}, and δ_{bs} are $0.057\%D$, $0.049\%D$, and $0.036\%D$, respectively.

• For H_d/H less than 0.7, no evidence can be shown to demonstrate that relationships exist between H_d/H and δ_{hm}, δ_{vm}, and δ_{bs} individually. However, for H_d/H more than 0.7, values of δ_{hm}, δ_{vm}, and δ_{bs} tend to decrease slightly. There is an evidence of a trend for increasing the embedment length, more soils under the excavation surface are strengthened disregarding the excavations with H_d/H less than 0.7. Consequently, less values of δ_{hm}, δ_{vm}, and δ_{bs} will occur.

5 Analysis of FE models

A three-dimensional finite element (FE) model was made practical through recent advances in computational capabilities, including the formulation of tieback-soil interaction and iterative solvers in the MSC.Marc 3D program. A range of factors may be influencing the ground surface movements and deformations, including approximations in the representation of stratigraphy, initial ground surface, top of the wall elevations, and estimation of the wall bending stiffness or rotation stiffness in the FE models. Several idealizations and simplifications were made to reduce the complexity of the 3D program without affecting the accuracy of the output. The FE models are depicted in Fig. 12. The results in Fig. 13 show the predictive values of δ_{hm}, δ_{hm}, and δ_{bs} seem to increase as the construction proceeded. The predictive values of δ_{hm}, δ_{hm}, and δ_{bs} are 66 mm, 52 mm, and 30mm, respectively, which are smaller than the observed values of 97 mm, 58mm, and 35mm, respectively. It can be seen that the numerical analyses are capable of describing accurately the measured δ_{hm}, δ_{hm}, and δ_{bs} variations throughout the

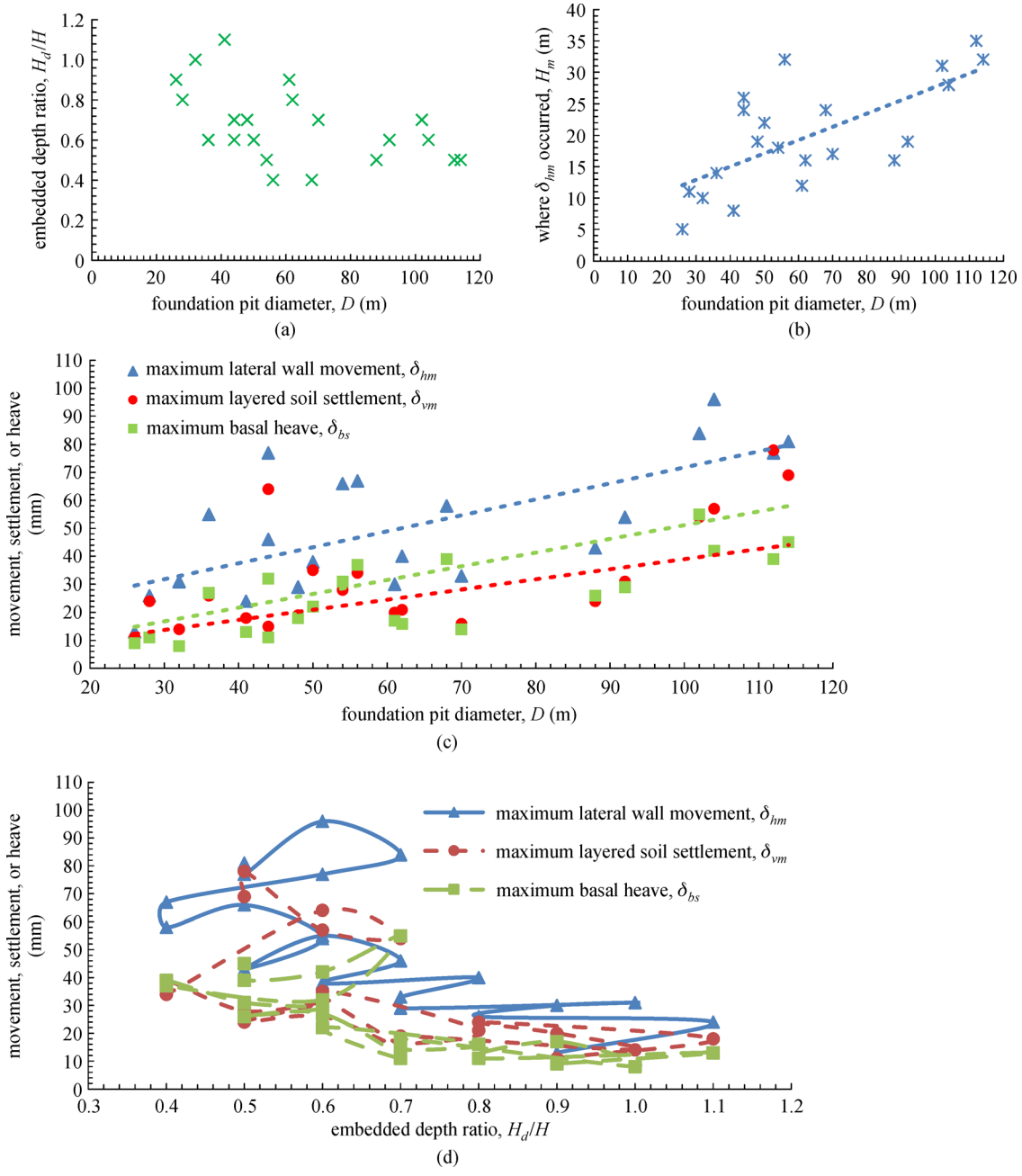

Fig. 11 (a) Embedded depth ratio H_d/H versus D ; (b) depth where δ_{hm} occurred versus D; (c) relationship between D and δ_{hm} , δ_{vm}, and δ_{bs}, respectively; (d) relationship between H_d/H and δ_{hm} , δ_{vm}, and δ_{bs}, respectively

construction process (six levels of struts) although the accuracy of the values may not be guaranteed. However, this simulation could be improved by considering some other complex factors. For example, analysis using a more complex soil model and accounting for partial drainage that spanned from November 22, 2009 to April 5, 2010 can be proposed as a further research.

6 Conclusions

To date, there is a scarcity of field data associated with deep excavations ($\geqslant$30 m) in soft soils for super high-rise buildings. The deep excavation for the foundation pit of the Shanghai Center provides a good opportunity to obtain valuable information related to observed ground surface movements and ground deformations during construction. On the basis of results of the ground monitoring and analysis presented herein, the major conclusions with regard to the performance of the Shanghai Center excavation are enumerated as follows:

1) The measured maximum lateral movement of the walls occurred at -18 m with a value $\delta_{hm} = 0.23\%H$ that is far below the upper boundary $\delta_{hm} = 1.0\%H$ [25], $\delta_{hm} =$

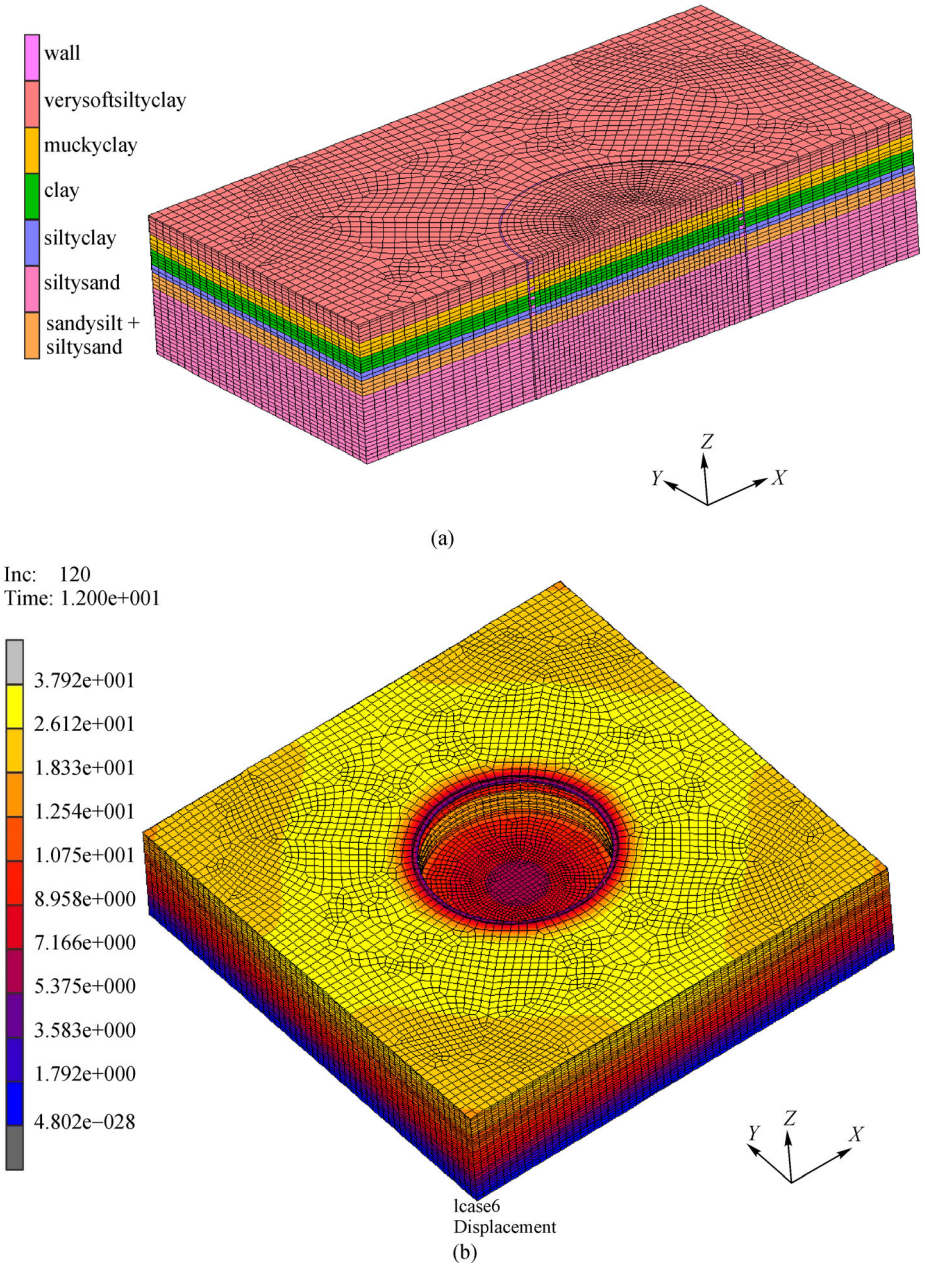

Fig. 12 The simulation models for estimating the ground movements and deformations duringconstruction process. (a) The site conditions of the FE model; (b) The basal heave at the last construction step (unit: cm)

$0.5\%H$ [20], and $\delta_{hm} = 0.6\%H$ [21]. The maximum lateral movement of the circumferential soils, δ_{hs}, occurred at-17 m, which deformed consistently with the walls. The locations of both δ_{hm} and δ_{hs} fall in the range between $H_m = H - 20$ and $H_m = H + 12$ that were proposed by Tan and Wang based on cylindrical excavations in Shanghai soft clay [3]. Contrary to the previous case studies, low embedment ratio 0.49 was adopted while no toe deflection emerged, which might be ascribed to the high stiffness of the retaining walls that were supported by six level struts to guarantee the stability of the excavation.

2) The layered settlement of the soils behind the walls is a common product of soil removal, ground lateral movements, and dewatering. The maximum soil settlement $\delta_{vm}/H = 0.172\%$ is within the range between $\delta_{vm}/H = 0.05\%$ and $\delta_{vm}/H = 0.20\%$ suggested by Hashash et al. based on the medium stiff Blue Clay of Boston [7]. The farther the distance between the street and the central pit, the lower ground settlement, thereby creating a funnel-shaped settlement profile for the ground settlement of the four surrounding streets. The maximum ground settlement was found at a distance of 20 m from the annex.

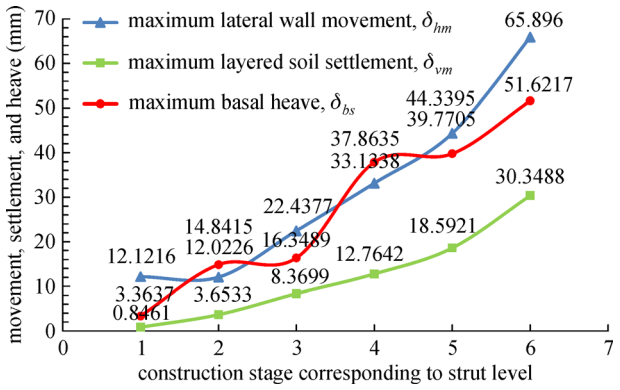

Fig. 13 The simulation results in different construction stage corresponding to each strut level

3) A great thick subsurface below the excavation bottom was involved to generate a heave for this deep excavation that was characterized by a decreasing tendency along the depth. The measured data indicated that the basal heave extended farther away from the excavation bottom than previously reported. The recorded maximum basal heave range between $\delta_{bh} = 0.15\%H$ and $\delta_{bh} = 0.16\%H$, which is much lower than that ranging between $\delta_{bh} = 0.30\%H$ and $\delta_{bh} = 0.90\%H$ [8]. A correlation between the maximum basal heave and the excavation diameter $\delta_{bh} = 0.04\%D$ is acquired. The heave generally decreased with the increase of the distance between the center of the pit and the measured point. Multiple factors (e.g., rebounding due to soil removal, consolidation induced by discharging of artesian water, suppression from soils outside of pit, and squeezing by retaining walls) may contribute to the heave development.

4) The results of the database analysis indicate that the average values of δ_{hm} δ_{vm}, and δ_{bs} increase with increasing the excavation depth and/or excavation diameter. There appears to be no discernible relationship between embedded depth ratio (H_d/H) and foundation pit diameter (D). For H_d/H more than 0.7, values of δ_{hm}, δ_{vm}, and δ_{bs} tend to decrease slightly due to the fact that more soils under the excavation surface would be strengthened by prolonging the embedded length of retaining walls.

5) FE models were established for estimating the ground surface movements and deformations throughout the construction process. The predictive values of δ_{hm}, δ_{hm}, and δ_{bs} are 66 mm, 52 mm, and 30 mm, respectively, which are smaller than the observed values due the fact that some complex factor are simplified. However, the numerical analyses are capable of describing accurately the measured variations of δ_{hm}, δ_{hm}, and δ_{bs}.

6) A retaining system was formed by combining the diaphragm walls and the circular struts in order to achieve an arching effect and bring compression resistance of concrete into full play. During the whole excavation, no big ground deflections that might lead to damage to the stability of the foundation pit were detected. This demonstrates that the construction sequence and excavation procedure (symmetrical, balanced, and layered) for this super foundation pit could guarantee the retaining system received minimal influence from the ground deformations.

Acknowledgements This paper is supported by National Natural Science Foundation of China (Grant No. 51768065). The field monitoring measurements used in this paper were made available to the writers through the efforts of many organizations and individuals involved with the construction and inspection of the foundation pit of the Shanghai Center project. Special thanks to SGIDI for facilitating access to field data. In addition, the writers would like to acknowledge the support of Ms. Yashuang Bai and Mr. Yuxia Ji for data compilation and figures processing. Any views and opinions expressed in this case study are those of the writers and do not necessarily represent the views of the organizations or other individuals responsible for the design and construction of this project.

Nomenclature

The following symbols are used in this paper:

γ: unit weight of soil (kN/m^3);

c': effective cohesion (kPa);

φ': effective friction angle (°);

v: Poisson's ratio (dimensionless unit);

K: permeability coefficient (10^{-4}cm/s);

$E_{m:}$ pressure meter modulus (MPa);

G_m: pressure meter shear modulus (MPa);

P_s: bearing capacity of static penetration test (MPa);

E: dynamic elastic modulus (MPa);

G: dynamic shear modulus (MPa);

H: excavation depth of the pit (m);

δ_{hm}: the maximum lateral movements of the walls (mm);

H_m: the depth whereδ_{hm} occurred (m);

D: foundation pit diameter (m);

H_d: embedded length of the retaining walls (m);

δ_{hs}: the maximum lateral movement of the circumferential soil (mm) ;

δ_{vm}: the maximum layered soil settlement (mm) ;

δ_{bs}: the maximum basal heave (mm).

References

1. Ou C Y, Liao J T, Lin H D. Performance of diaphragm wall constructed using the top-down method. Journal of Geotechnical and Geoenvironmental Engineering, 1998, 124(9): 798–808
2. Liu G B, Ng C W, Wang Z W. Observed performance of a deep multistrutted excavation in Shanghai soft clays. Journal of Geotechnical and Geoenvironmental Engineering, 2005, 131(8): 1004–1013
3. Tan Y, Wang D. Characteristics of a large-scale deep foundation pit excavated by the central-island technique in Shanghai soft clay. II: top-down construction of the peripheral rectangular pit. Journal of

Geotechnical and Geoenvironmental Engineering, 2013a, 139(11): 1894–1910

4. Whittle A J, Corral G, Jen L C, Rawnsley R P. Predication and performance of deep excavations for Courthouse Station, Boston. Journal of Geotechnical and Geoenvironmental Engineering, 2015, 141(4): 04014123
5. Orazalin Z Y, Whittle A J, Olsen M B. Three-dimensional analysis of excavation support system for the Stata Center Basement on the MIT campus. Journal of Geotechnical and Geoenvironmental Engineering, 2015, 141(7): 05015001
6. Tanner Blackburn J, Finno R J. Three-dimensional responses observed in an internally braced excavation in soft clay. Journal of Geotechnical and Geoenvironmental Engineering, 2007, 133(11): 1364–1373
7. Hashash Y M A, Osouli A, Marulanda C. Central artery/tunnel project excavation induced ground deformations. Journal of Geotechnical and Geoenvironmental Engineering, 2008, 134(9): 1399–1406
8. Tan Y, Wang D. Characteristics of a large-scale deep foundation pit excavated by the central-island technique in Shanghai soft clay. I: bottom-up construction of the central cylindrical shaft. Journal of Geotechnical and Geoenvironmental Engineering, 2013b, 139(11): 1875–1893
9. Wong I, Poh T, Chuah H. Performance of excavations for depresses expressway in Singapore. Journal of Geotechnical and Geoenvironmental Engineering, 1997, 123(7): 617–625
10. Hsieh P G, Ou C Y. Shape of ground surface settlement profiles caused by excavation. Canadian Geotechnical Journal, 1998, 35(6): 1004–1017
11. Long M. Database for retaining wall and ground movements due to deep excavations. Journal of Geotechnical and Geoenvironmental Engineering, 2001, 127(3): 203–224
12. Moormann C. Analysis of wall and ground movements due to deep excavations in soft soil based on a new worldwide database. Soil and Foundation, 2004, 44(1): 87–98
13. O'Rourke T D, McGinn A J. Lessons learned for ground movements and soil stabilization from the Boston Central Artery. Journal of Geotechnical and Geoenvironmental Engineering, 2006, 132(8): 966–989
14. Wang J H, Xu Z H, Wang W D. Wall and ground movements due to deep excavations in Shanghai soft soils. Journal of Geotechnical and Geoenvironmental Engineering, 2010, 136(7): 985–994
15. Tan Y, Wei B. Observed behaviors of a long and deep excavation constructed by cut-and-cover technique in Shanghai soft clay. Journal of Geotechnical and Geoenvironmental Engineering, 2012, 138(1): 69–88
16. Tan Y, Wang D. Structural behaviors of large underground earth-retaining systems in Shanghai I: unpropped circular diaphragm wall. Journal of Performance of Constructed Facilities, 2015a, 29(2): 04014058
17. Tan Y, Wang D. Structural behaviors of large underground earth-retaining systems in Shanghai. II: multipropped rectangular diaphragm wall. Journal of Performance of Constructed Facilities, 2015b, 29(2): 04014059
18. Shanghai Construction and Management Commission. Code for Investigation of Geotechnical Engineering (DGJ08-37-2002), Shanghai: Jian Zhu Jian Cai Ye Shi Chang Guan Li Zong Zhan, 2002 (in Chinese)
19. Xu Y S, Shen S L, Du Y J. Geological and hydrogeological environment in Shanghai with geohazards to construction and maintenance of infrastructures. Engineering Geology, 2009, 109(3–4): 241–254
20. Clough G W, O'Rourke T D. Construction induced movements of in-situ walls. Geotechnical Special publication: Design and performance of earth retaining structures (GSP25), ASCE, Reston, VA, 1990
21. Kung G T C, Juang C H, Hsiao E C L, Hashash Y M A. Simplified model for wall deflection and ground-surface settlement caused by braced excavation in clays. Journal of Geotechnical and Geoenvironmental Engineering, 2007, 133(6): 731–747
22. Liu K X. Three dimensional analysis of deep excavation in soft clay. M.Eng. thesis, National University of Singapore, 1995
23. Lee F, Yong K, Quan K, Chee K. Effect of corners in strutted excavations: field monitoring and case histories. Journal of Geotechnical and Geoenvironmental Engineering, 1998, 124(4): 339–349
24. Liu G B, Jiang R J, Ng C, Hong Y. Deformation characteristics of a 38m deep excavation in soft clay. Canadian Geotechnical Journal, 2011, 48(12): 1817–1828
25. Peck R B. Deep excavation and tunneling in soft grund. In: Proceedings of the 7th International Conference of Soil Mechanics and Foundation Engineering, Mexico City, 1969, 225–281